Journal of Power Sources 226 (2013) 156–161

Contents lists available at SciVerse ScienceDirect

Journal of Power Sources

journal homepage: www.elsevier.com/locate/jpowsour

Effects of acidity and alkalinity on corrosion behaviour of Al–Zn–Mg based anode alloy

Jingling Ma*, Jiuba Wen, Quanan Li, Qin Zhang

School of Materials Science and Engineering, Henan University of Science and Technology, Luoyang 471003, PR China

HIGHLIGHTS

- The corrosion kinetic of the alloy is minimized in slightly neutral solution.
- In acidic or neutral solution, general and pitting corrosion occurred simultaneously.
- In alkaline solution, the alloy mainly suffered general corrosion.
- The alloy undergoes two types of pitting: hemispherical and crystallographic.

ARTICLE INFO

Article history:
Received 14 August 2012
Received in revised form
21 October 2012
Accepted 22 October 2012
Available online 29 October 2012

Keywords:
Aluminium alloy
Corrosion
Potentiodynamic and cyclic polarization curves
pH

ABSTRACT

Effects of 1 M HCl, 0.6 M NaCl with different pH values and 4 M NaOH solutions on the corrosion behaviour of Al–5Zn–1Mg–0.02In–0.05Ti–0.5Mn (wt%) alloy have been investigated using measurements of self-corrosion, potentiodynamic polarization, cyclic polarization experiment combined with open circuit potential technique and scanning electron microscopy. The corrosion behaviour of the alloy was found to be dependant on the Cl^-, OH^- ions and pH value. In acidic or slightly neutral solutions, general and pitting corrosion occurred simultaneously. In contrast, exposure to alkaline solutions results in general corrosion which was traced back to the dissolution of the resistive oxidation film on the surface of the alloy. Experience revealed that the alloy was susceptible to pitting corrosion in all chloride solution. The alloy undergoes two types of localized corrosion process, leading to the formation of hemispherical and crystallographic pits. Polarization resistance measurements which are in good agreement with those of self-corrosion, show that the corrosion kinetic is minimized in slightly neutral solutions (pH = 7).

1. Introduction

Because of the low atomic mass of aluminium, high energetic capacity (2980 Ah kg^{-1}), along with the negative value of standard electrode potential (−1.66 V vs. NHE), low cost, and no pollution, Al-air battery is a promising power source and energy storage device [1–3]. However currently, the Al-air battery is still not as popular as Zn-air battery [4]. The major problem is that Al anode exhibited some less attractive properties, such as the protective oxide film, which is spontaneously formed on Al surface in air and in aqueous solutions, and severe self-corrosion during battery discharge [5,6]. Due to presence of oxide film, the corrosion potential of Al electrode is shifted in the positive direction (almost for −0.8 V vs. NHE), and the active dissolution of Al is slowed down considerably [7,8]. The addition of alloying elements such as In, Ga, Hg, Sn shifts the potential towards more negative potentials, causing the so-called activation of Al [9–11]. This wasteful self-corrosion resulted in severe capacity loss and low anodic efficiency, and these disadvantages have delayed the development of Al-air battery and limited its commercial exploitation. For the purpose of reducing the self-corrosion of Al alloys the measures were taken: use alloying with the elements of high hydrogen overpotential such as Pb, Zn and Sn, etc [12–16]. The paper [17] investigated the effects of Mg and Ti on microstructure and electrochemical performance of Al–Zn–In alloy. The Al–Zn–Mg–In–Ti series anodes have become popular in China [18,19]. In order to further reduce the self-corrosion of the alloy, it is necessary reducing the harmful effects of impurity Fe element. Mn element can be come into being Al_6(Mn, Fe) in the alloy and the potential of Al_6(Mn, Fe) is almost the same with that Al based, thereby reducing the harmful effects of the impurities Fe [20,21]. Thus the Al–5Zn–1Mg–0.02In–0.05Ti–0.5Mn anode is developed.

* Corresponding author. Tel.: +86 13698854177; fax: +86 379 64231846.
E-mail address: majingling.student@sina.com (J. Ma).

0378-7753/$ – see front matter © 2012 Elsevier B.V. All rights reserved.
http://dx.doi.org/10.1016/j.jpowsour.2012.10.075

The high dissolution rate of aluminium in the concentrated alkaline solutions is known to stem from the attack by hydroxyl ions in the solution [22]. It has been reported that the addition of Cl^- ions to acidic and neutral solutions increases the anodic dissolution rate of aluminium [23,24]. The paper [25] investigated the corrosion behaviour of Al–5Zn–1Mg–0.02In–0.05Ti–0.5Mn alloy in 3.5% NaCl solution. However, it provides little information about the anodic dissolution of the alloy in acidic and alkaline solution. The present work is aimed to study the corrosion behaviour of the alloy in acidic and alkaline solution and different pH of NaCl solutions. The effect of the pH solutions and the potentiodynamic anodic polarization on the localized corrosion of the alloy will be considered.

2. Experimental

2.1. Material preparation

The nominal compositions of alloy in present experiment are 5% wt Zn-1%wt Mg-0.02% wt In-0.05% wt Ti-0.5% wt Mn–Al. Raw materials are commercial pure aluminium, zinc, indium, magnesium, titanium, manganese ingots (>99.9%) for casting the above anode alloy. Raw material ingots were cut, dried, weighed the required amount of materials and melted in a graphite crucible in ZGJL0.01-4C-4 vacuum induction furnace under argon atmosphere at 760 °C. The molten alloy was poured in a preheated cast iron dye. The ultimate composition of the alloy was analyzed by direct reading spectrometer, and the result is shown in Table 1.

2.2. Electrochemical measurements

The electrochemical tests were carried out with three electrodes system at room temperature by CHI660C electrochemical test system (CHI Company, USA). A saturated calomel electrode (SCE) served as the reference electrode and a Pt sheet was used as the counter electrode.

The working electrodes of open circuit potentials measured with an exposed area of 1 cm^2. The samples were ground with emery paper (grade 400–800–1000–2000) and then cleaned with triply distilled water. Measurements were performed in these solutions for 1 h.

The electrolytes used in this study were 4 M NaOH solutions, 0.6 M NaCl solutions and 1 M HCl solutions. All solutions were prepared with distilled water and analyticalgrade reagents. NaCl was added to the distilled water in requisite amount to make a solution with concentration 0.6 M (3.5 wt%) NaCl. The pH of the solutions was adjusted by using analyticalgrade reagent sodium hydroxide (NaOH) and hydrochloric acid (HCl). All of the pH measures were made by mean of pH-metre.

The potentiodynamic polarization was measured at a scan rate of 1 mV s^{-1} by CHI660C electrochemical test system after Pt sheet and the sample electrodes were suspended in solutions for 1 h. Several polarization tests were performed on each of the samples to build up a representative indication of the corrosion behaviour.

2.3. Self-corrosion

The samples of self-corrosion tests were cut to ¢ 11.4 mm × 5 mm. The samples were ground with emery paper (grade 400–800–1000–2000) and immersed in different solutions for 24 h. The weight of the samples before and after immersion was measured after cleaning the corrosion products formed on the sample surface. The corrosion products of the samples were cleaned out in solutions of 2% CrO_3 and 5% H_3PO_4 at 80 °C for about 5 min, then rinsed by ethanol.

The corrosion rate was calculated using the formula:

$$\text{Corrosion rate} = \text{Weight loss/ surface area/ time of immersion}\left(\text{mg cm}^{-2}\ \text{min}^{-1}\right)$$

The anode surface after corrosion or polarization was examined using JSM-5610LV scanning electron microscope (SEM).

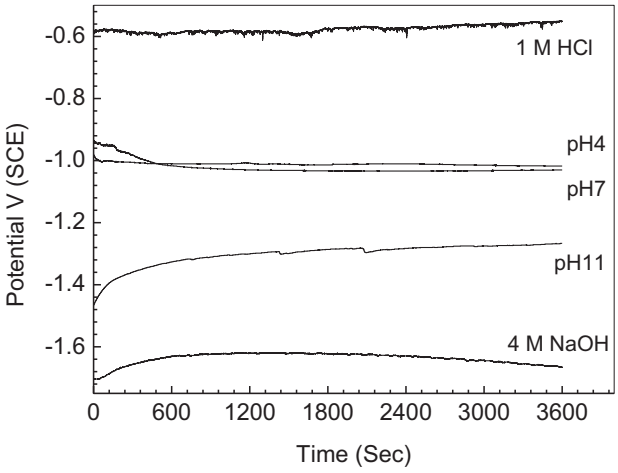

Fig. 1. Evolution of the open circuit potential vs. time in different solutions for samples of the alloy.

3. Results and discussion

3.1. Open circuit potential (OCP)

Fig. 1 shows the OCP vs. time curves obtained with samples immersed in different solutions. Several OCP tests were performed on each of the samples to build up a representative. It can be seen that the OCP of the samples is observed to change more negative potentials with pH increasing. The curves clearly show that, in the acidic and neutral solutions, the studied material exhibited a relatively stable steady open circuit potential around −1000 mV. In contrast to this, exposure to 1 M HCl, pH 11 and 4 M NaOH alkaline solutions results in relatively stable steady open circuit potential around −576 mV, −1274 mV and −1666 mV, respectively. This process is partially dependant on the electrolyte chemical composition [26,27].

3.2. Self-corrosion rate

The weight loss of samples in different solutions for 24 h immersion was obtained from the difference between weight of the samples before and after immersion. Table 2 shows the values of the self-corrosion rate from the loss of weight by unit of surface

Table 1
Chemical compositions of the studied alloy (wt%).

Element	Zn	Mg	In	Ti	Mn	Fe	Cu	Si	C	Al
Composition	5.020	0.904	0.024	0.035	0.436	<0.001	0.032	0.062	0.051	Remainder

Table 2
Self-corrosion rate of the studied alloy in different solutions.

Solutions	Initial mass/g	Mass after corrosion/g	Weight loss/mg	Corrosion rate/mg cm^{-2} h^{-1}	Corrosion rate/cm $year^{-1}$
1 M HCl	0.8722	0.8163	55.9	2.392	7.754
pH 4	0.8104	0.809	1.4	0.062	0.195
pH 7	1.0524	1.0519	0.5	0.022	0.065
pH 11	0.5063	0.5045	1.8	0.075	0.227
4 M NaOH	0.9998	0.0709	928.9	38.473	124.814

Table 3
Corrosion parameters of the studied alloy in Fig. 2.

Solutions	R_p/Ω	I_{corr}/A cm^{-2}
1 M HCl	236	1.428×10^{-4}
pH 4	7834	2.44×10^{-6}
pH 7	10,063	2.33×10^{-6}
pH 11	1968	1.050×10^{-5}
4 M NaOH	5	9.348×10^{-3}

area, corresponding to samples of the alloy submitted to immersion tests of 24 h. The results from this table demonstrate that, when the alloy is submitted to immersion in neutral solutions, a decrease is produced in the weight loss, self-corrosion rate, and an increase is seen in this if the values of the pH are displaced in acidic or alkaline. In other words, there is an increase in the alloys susceptibility to corrosion in the acidic and alkaline solutions.

The results obtained above can be interpreted by considering the fact that the chemical reactions of aluminium alloy are unusual in the sense that these materials are amphoteric, i.e., soluble in acid as well as in alkali solutions [28]. In acidic solution, the solubility of Al^{3+} facilitates the dissolution of the Al matrix and further accelerates the chloride attack. However, the corrosion mechanism of aluminium alloy in neutral and alkaline media is related with the formation of protective layer of aluminium hydroxides $Al(OH)_3$. The oxide film is uniformly thinned by the chemical dissolution, which is facilitated by the presence of high OH^- concentration in alkaline solution [29]. Whereas in neutral solutions, the passive film of aluminium hydroxides ($Al(OH)_3$) formed on alloy surface is remarkably stable due to its low solubility, acts as protector for this alloy against corrosive agents.

3.3. Potentiodynamic polarization

Fig. 2 shows typical potentiodynamic polarization curves for the samples, obtained in different solutions. A similar shape is observed in two polarization curves which were obtained in pH 4 and pH 7 solutions, with a little difference on their cathodic branch controlling the corrosion process, indeed the current density in pH 7 solutions is the lowest. The onset of pitting is not visible in these two cases since the pitting potentials E_{pit} coincided with the corrosion potentials E_{cor}. From these results, it can be concluded that the main corrosion mechanism in these solutions of pH values 4 and 7 is pitting corrosion and the pitting potential is independent of pH over this pH range [30].

On the contrary, in case of alkaline solutions (pH = 11), the values of corrosion potential E_{cor} were observed to be lowered to more cathodic values, from −1012 mV to −1271 mV without a change in the pitting potential. Further, the decrease in the corrosion potential E_{cor} values, compared to those of pH 4 and neutral pH, indicate the loss of passivity of the alloy due either to thinning of surface oxide layer by hydroxide ion (OH^-) attack (alkaline chemical dissolution) or to the absence of the primary oxide film [31].

However, by increasing the solution pH, the pitting potential remained unchanged, a separation of the E_{cor} from the pitting potential ($E_{pit} - E_{cor}$) was observed from the polarization curves of

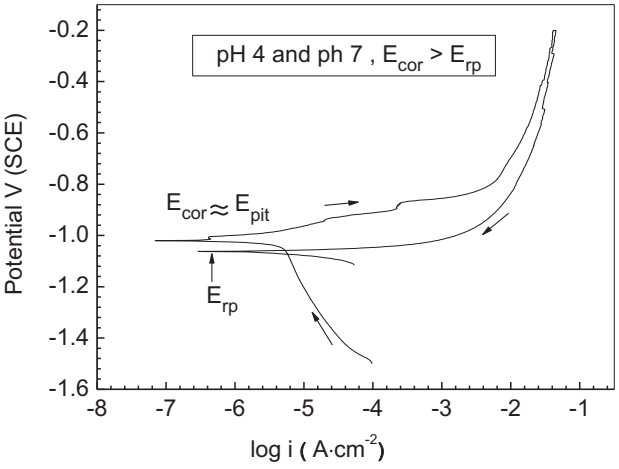

Fig. 3. Cyclic polarization curve obtained with the alloy in solutions of 0.6 M NaCl at pH = 7 (this curve is similar to that of pH = 4).

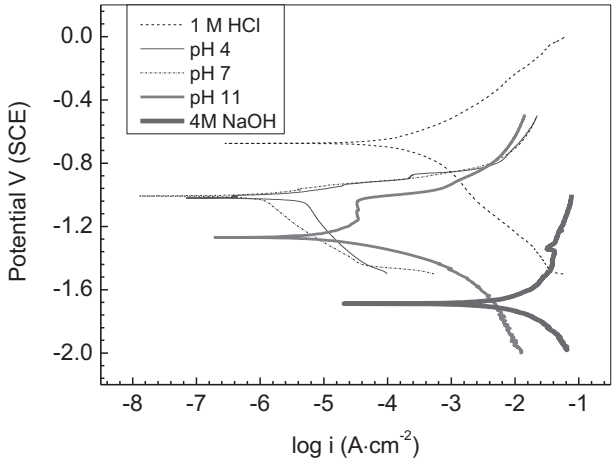

Fig. 2. Polarization curves obtained with samples of the alloy in solutions of 1 M HCl, 0.6 M NaCl at pH = 4, at pH = 7 and 4 M NaOH.

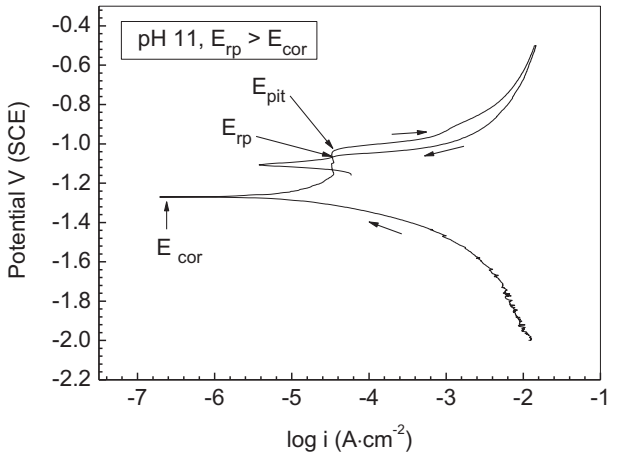

Fig. 4. Cyclic polarization curve obtained with a samples of the alloy in solutions of 0.6 M NaCl at pH = 11.

Fig. 2 and at the same time, anodic current density plateau region was formed below the pitting potential E_{pit}. The reasonable value of the anodic current density within this plateau region (3.16×10^{-5} A cm^{-2}), which may presumably arise from either the charge transfer reaction at the electrolyte/oxide film interface or the Al^{3+} ion transport through the oxide film [32].

Comparing the cathodic branches of the polarization curves for this system in different solutions, it can be observed that, while the samples in 1 M HCl acidic solutions and 4 M NaOH alkaline media show high cathodic current densities $I_{cathodic}$, the samples of the alloy exhibit a low cathodic current density $I_{cathodic}$ at slightly neutral pH 7 media (Fig. 2). Further, the cathodic current density $I_{cathodic}$ of this system, which is equivalent to corrosion rate, is found to be in the order 4 M NaOH > 1 M HCl > pH 11 > pH 4 > pH 7. This result agrees well with the preceding one.

A similar result to the above one were drawn from the analysis of the values of polarization resistance (R_p) and exchange current density ($I_{corrosion}$) calculated from the corresponding polarization curves recorded for samples of the alloy exposed to different solutions (Table 3). Thus, in Table 3 the values of R_p and I_{corr} of different solution are represented.

The results from this table clearly demonstrate that, the polarization resistance (R_p) of the alloy was found to be a maximum in the slightly neutral pH 7 solutions (about $1.0 \times 10^4\ \Omega$). Furthermore, in this table it can be appreciated how, in line with the results of self-corrosion rate measurements, there is a fall in the polarization resistance R_p values, and accordingly an increase in the dissolution activity of the system when the pH of solution was displaced in acidic or in alkali values. This fact is consistent with the maximum self-corrosion rate of the alloy in alkali solution and a minimum self-corrosion rate in slightly neutral pH 7 solutions, as it can be observed in Table 2. Assuming the alloy density similar to that for pure Al of 2.7 g cm^{-3}, the corrosion rate translates to a linear penetration rate and shown in Table 2. The lowest rate of

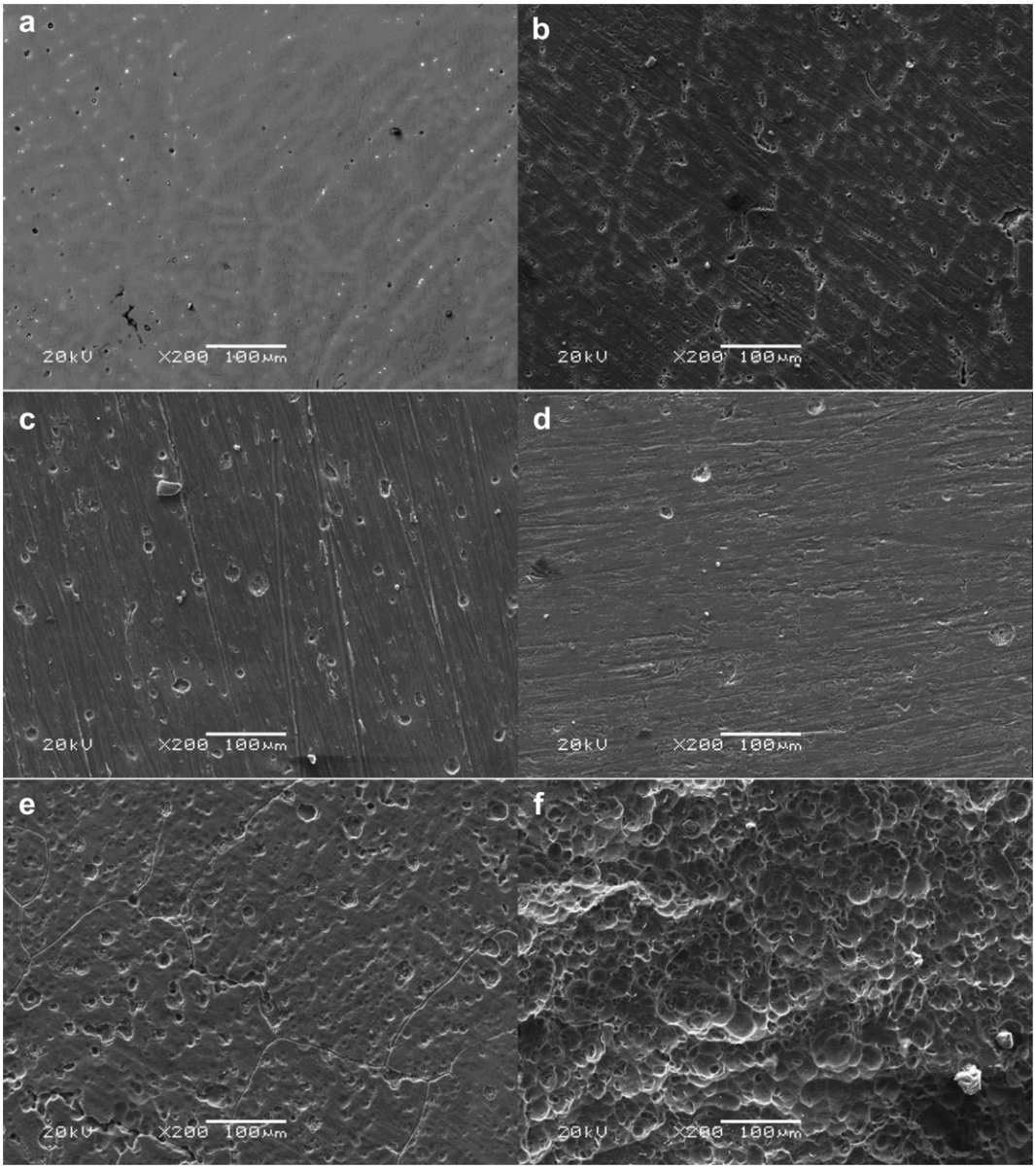

Fig. 5. Micrograph of sample polished to mirror quality (a), and corrosion morphology of samples after 24 h immersion in different solutions: 1 M HCl (b), pH 4 (c), pH 7 (d), pH 11 (e) and 4 M NaOH (f).

0.065 cm year^{-1} (pH 7 NaCl) is too high for a practical metal air anode. So, the alloy is unsuitable as an cells.anode in a power producing aluminium air

3.4. Cyclic polarization

One of the tests to assess the susceptibility of the alloy to localized corrosion and passive stability was the cyclic potentiodynamic polarization technique at low scan rate. Pitting susceptibility can be predicted fairly reliably from the anodic portion of a scan. If the reverse anodic curve is shifted to lower currents (negative hysteresis) or if the reverse curve essentially retraces the ascending curve (neutral hysteresis), no pitting is expected. In contrast, if the reverse anodic curve is shifted to higher currents than the forward curve (positive hysteresis), pitting is expected.

A typical cyclic potentiodynamic polarization curve obtained for the alloy in contact with 0.6 M NaCl solutions having slightly neutral pH 7 was shown in Fig. 3. The solid arrows next to the forward and the reverse anodic branches indicate potential scan directions. The alloy did not show a classical passive region with the current density totally independent of applied potential. Fig. 3 shows an example of positive hysteresis, with pitting potential located at the same position of that of corrosion potential, repassivation potential E_{rp} less than the E_{cor} and large area of the hysteresis loop, suggesting the nucleation and growth of pitting during the reverse scan [33]. In general, the larger the area of the hysteresis loop is, the greater the susceptibility of the material to pitting corrosion. After the tests, the examined samples of the alloy showed the same morphology of the attack by pitting.

Fig. 4 shows the cyclic potentiodynamic polarization for the alloy sample in aqueous solution at pH = 11. The material showed a classical passive region with the current density practically independent of applied potential up to pitting potential $E_{pit} = -1035$ mV. Then, the current density increased abruptly until reaching certain value after that it continue to increase very slightly with increasing potential and the reverse polarization curve showed a positive hysteresis, suggesting the nucleation and growth of pitting corrosion at the point of potential breakdown (E_{pit}). Although, the pitting corrosion was preceded by uniform thinning of the oxide film and uniform dissolution overwhelmed the pitting corrosion.

3.5. Morphology of corrosion attack

Fig. 5a presented microstructure for the alloy and polished to mirror quality. This micrograph is presented here for comparison with those of corroded samples. In this figure, the alloy is mainly consisted of α-Al matrix with tiny precipitates. Fig. 5b–d shows the micrograph of the surface of the sample after 24 h immersion in 1 M HCl solutions, 0.6 M NaCl solutions at acidic pH (pH = 4) and slightly neutral (pH = 7) respectively. Hemispherical pits with different size were grown throughout the surfaces of the samples as the result of the corrosion of the alloy matrix in the vicinity of the precipitates. Attack with similar morphology has been reported by other authors as localized alkaline corrosion [34].

These micrographs clearly show that the damage caused by this type of corrosion is accentuated in solutions of acidic pH comparing to slightly neutral solution, suggesting that the anodic activity of the system became intense with this acid range of pH. Exposure to solutions of alkaline pH results in more intense corrosion attack. Fig. 5e and f shows the morphology of the sample surface immersed in 0.6 M NaCl at pH = 11 and 4 M NaOH solutions for 24 h.

SEM micrograph of the corroded surfaces of the alloy after the potentiodynamic polarization shows a novel morphology which is considerably different from that produced by immersion

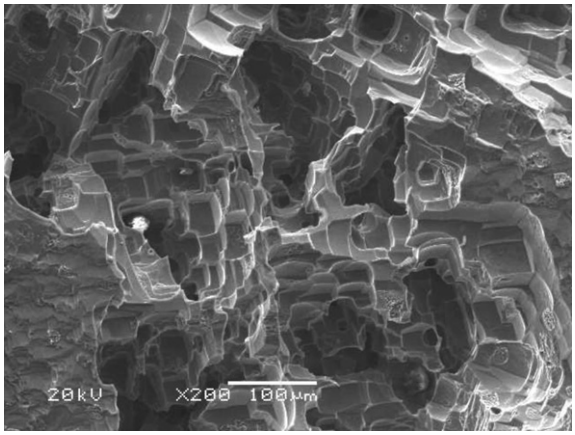

Fig. 6. SEM micrograph of sample after potentiodynamic anodic polarization in 4 M NaOH solutions.

experiments. As can be observed in Fig. 6, the treatment of the alloy samples using potentiodynamic anodic polarization leads to the formation of crystallographic pitting, similar to that described by Brunner et al. [35] for pure aluminium and aluminium alloys. The presence of some of geometric facets can be explained by the fact that the attack occurs probably according to well defined crystallographic directions [36].

The SEM micrographs (Figs. 5 and 6) of the corroded surfaces of the alloy after immersion tests and potentiodynamic polarization experiments strongly support the above electrochemical features.

4. Conclusions

This paper describes a study conducted on the effects of 1 M HCl solutions, 4 M NaOH and with different pH NaCl solutions on the corrosion behaviour of Al–5Zn–1Mg–0.02In–0.05Ti–0.5Mn alloy. The corrosion behaviour of the alloy was found to be dependant on the acidity and alkalinity of solutions. The results obtained by self-corrosion rate, that the alloy undergoes a corrosion process due to intense chemical dissolution by OH^- in alkaline solutions and at relatively low degree in acidic solution. This means that this material exhibit a notable corrosion resistance in neutral chloride solutions which is well validated by R_p and I_{corr} measurement.

The potentiodynamic polarization curves showed that the pitting potential E_{pit} is independent of the pH value. The curves showed also, that an increase in the pH shifts the corrosion potential E_{cor} to more active values and enlarges the width of the passive region below the pitting potential E_{pit}. This clearly means that uniform thinning of the initial oxide through the chemical dissolution by hydroxide OH^- ion attack dominates over the pitting corrosion by chloride Cl^- ion attack, which is well validated by the cyclic potentiodynamic polarization curves.

Experience revealed that the alloy undergoes two types of localized corrosion process, leading to the formation of hemispherical and crystallographic pitting. Hemispherical pitting is found to occur on the surface of this material under a simply exposure in chloride solution whereas for the formation of the crystallographic pits, it is necessary to polarize the alloy.

Acknowledgement

This work was supported by Cultivation Research Innovation Ability of Henan University of Science and Technology (Grant No. 2012ZCX017), Innovative Research Team (in Science and Technology) in University of Henan Province (Grant No.

2012IRTSTHN008) and Science and Technique Key Program of He'nan Educational Committee (Grant No. 12A430007).

References

[1] S.H.H. Yang, H. Knickle, J. Power Sources 112 (2002) 162–173.
[2] H. Wu, World Non-Grid-Connected Wind Power Energy Conf. (2010) 245–248.
[3] Z.A. Zhuk, E.A. Sheindlin, V.B. Kleymenov, I.E. Shkolnikov, Y.M. Lopatin, J. Power Sources 157 (2006) 921–926.
[4] G.M. Wu, C.C. Yang, J. Membr. Sci. 280 (2006) 802–808.
[5] F. Reichel, L.P.H. Jeurgens, E.J. Mittemeijer, Acta Mater. 12 (2008) 2897–2907.
[6] Z.Q. Ma, X.X. Li, J. Solid State Electr. 15 (2011) 2601–2606.
[7] S. Gudic, I. Smoljko, M. Kliškic, Electrochim. Acta 50 (2005) 5624–5632.
[8] M.A. Amin, E.R. Abd, S. Sayed, E.F. Essam, R.S. Mahmoud, N.M. Abbas, Electrochim. Acta 54 (2009) 4288–4296.
[9] S.E.A. Zein, A.Q. Saleh, J. Appl. Electrochem. 34 (2004) 331–339.
[10] W. Xiong, G.T. Qi, X.P. Guo, Z.L. Lu, Corros. Sci. 53 (2011) 1298–1303.
[11] A. Elango, V.M. Periasamy, M. Paramasivam, Anti-Corros. Methods Mater. 56 (2009) 266–272.
[12] S.A. Mideen, M. Ganesan, M.A. Athan, K.B. Sarangapani, V. Balaramachandran, V. Kapali, S.V. Iyer, J. Power Sources 27 (1989) 235–244.
[13] I. Herraiz-Cardona, E. Ortega, V. Pérez-Herranz, Electrochim. Acta 56 (2011) 1308–1315.
[14] C. Blawert, C.D. Fechner, D. Höche, V. Heitmann, W. Dietzel, K.U. Kainer, P. Zivanovic, C. Scharf, A. Ditze, J. Gröbner, R. Schmid-Fetzer, Corros. Sci. 52 (2010) 2452–2468.
[15] S. Valdez, J. Genesca, B. Mena, J.A. Juarez-Islas, J. Mater. Civ. Eng. 10 (2001) 596–604.
[16] C.M. Quevedo, J. Genesca, NACE Int. Corros. Conf. Ser. (2008) 080521.
[17] J.L. Ma, J.B. Wen, X.D. Li, S.L. Zhao, Y.F. Yan, Rare Met. 28 (2009) 187–192.
[18] H. Sinaa, M. Emamya, M. Saremia, A. Keyvania, M. Mahtaa, J. Campbellb, Mater. Sci. Eng. A 431 (2006) 263–272.
[19] W.D. Ren, J.F. Li, Z.Q. Zheng, Trans. Nonferrous Met. Soc. China 17 (2007) 727–732.
[20] P. Ratchev, B. Verlinden, P. Van Houtte, Acta Metall. Mater. 43 (1995) 621–629.
[21] D.T. Alexander, A.L. Greer, Acta Mater. 50 (2002) 2571–2583.
[22] D. Mercier, M.G. Barthés-Labrousse, Corros. Sci. 51 (2009) 339–348.
[23] B. Zaid, D. Saidi, A. Benzaid, S. Hadji, Corros. Sci. 50 (2008) 1841–1847.
[24] Y. Liu, G.Z. Meng, Y.F. Cheng, Electrochim. Acta 54 (2009) 4155–4163.
[25] J.L. Ma, J.B. Wen, J. Alloys Compd. 496 (2010) 110–115.
[26] M. Janik-Czachor, Corrosion 49 (1993) 763–769.
[27] W.S. Tait, K.A. Handrich, Corrosion 50 (1994) 373–380.
[28] E. Deltombe, M. Pourbaix, Corrosion 14 (1958). 496–453.
[29] H.R. Zhou, X.G. Li, J. Ma, C.F. Dong, Y.Z. Huang, Mater. Sci. Eng. B 162 (2009) 1–8.
[30] A.A. Mohammed, Electrochim. Acta 54 (2009) 1857–1863.
[31] Y. Liu, M.A. Arenas, S.J. Garcia-Vergara, T. Hashimoto, P. Skeldon, G.E. Thompson, H. Habazaki, P. Bailey, T.C.Q. Noakes, Corros. Sci. 50 (2008) 1475–1480.
[32] O. Guseva, P. Schmutz, T. Suter, O.V. Trzebiatowski, Electrochim. Acta 54 (2009) 4514–4524.
[33] A.A. Mohammed, S.A. Sayed, E.F. El-Sherbini, N.A. Mohsen, Electrochim. Acta 54 (2009) 4288–4296.
[34] A. Boag, A.E. Hughes, A.M. Glenn, T.H. Muster, D. McCulloch, Corros. Sci. 53 (2011) 17–26.
[35] J.G. Brunner, J. May, H.W. Höppel, M. Göken, S. Virtanen, Electrochim. Acta 55 (2010) 1966–1970.
[36] K.L. Moore, J.M. Sykes, P.S. Grant, Corros. Sci. 50 (2008) 3233–3240.